

## **NONDESTRUCTIVE EVALUATION OF CEMENT-BASED MATERIALS WITH COMPUTER VISION**

S. Choi,  
Harbor Engineering Lab., Korea Ocean Research & Development Institute,  
Ansan, Korea  
S. P. Shah,  
Center for ACBM, Northwestern University, Evanston IL, USA

### **Abstract**

Nonlinear behavior in the pre-peak and strain-softening phenomenon can be explained in terms of microcracks and macrocracks. Numerous microstructural features that absorb energy make concrete a quasi-brittle material. Microcracks form at relatively low stresses, and as the stress increases, the microcracks tend to localize into macrocracks that ultimately lead to specimen failure. Experiments to study the compressive fracture of cement-based materials were conducted. The permeability or durability of concrete is directly related to the formation of microcracks, and thus accurate observation is essential. Microcracks, which are the precursors of macrocracks, form at early stages of stress and cannot be easily detected due to small sizes. Computer vision, which is based on digital image correlation, was used to measure microcrack openings. The authors dramatically improved the accuracy by increasing the image resolution.

The microcrack propagation near aggregates was examined with subregion scanning computer vision. The formation of cracks were monitored through several loading steps. Nonuniform local displacements were observed with different end conditions as well as with different material composition.

Key words: NDE, concrete fracture, computer vision

## **1 Introduction**

The initial formation and growth of microcracks have been important issues in dealing with the compressive fracture of quasi-brittle materials like concrete. Many nondestructive evaluation techniques such as acoustic emission, laser holography, moiré interferometry, electronic speckle pattern interferometry, and x-ray microtomography have been used (Jia and Shah, 1994; Shao et al., 1993; Maji et al., 1991). Nonetheless microcracks cannot be easily measured due to various technical difficulties such as the complexity of crack patterns, the vibration of testing machines, and small opening of microcracks. Computer vision (or digital image correlation) was used to detect and measure cracks. With this method, multiple cracks, which are common in compressive failure - can be examined without problematic technical limitations. Also, automated computation of displacements does not require laborious processes, and it is especially helpful when a large quantity of specimens are examined. The authors have dramatically improved the accuracy by increasing image magnification factor. This method, subregion scanning computer vision (SSCV), was applied to the study of compressive behavior of concrete.

## **2 Compressive fracture of cement-based materials**

### **2.1 Experimental stability and sensitivity of failure**

It is important to obtain a well-controlled stable softening branch in the study of failure localization. It is also essential to acquire clear images at desirable loading stages for computer vision. There are several issues in obtaining the descending portion of a load-displacement curve. First of all, the magnitude of stiffness for a testing machine should be bigger than that of a specimen to overcome the stability problem (Hudson et al., 1972; Wang et al., 1978). Another one is that the frequency response of the testing system should also be faster than the energy release rate of a specimen. Otherwise, unstable progress of failure can not be avoided (Hillerborg, 1989). At the same time, a suitable feedback signal in conjunction with a closed-loop servo controlled testing machine should be chosen. A combined feedback signal, which mixes two different signals has been used by several researchers to obtain stable and controlled post-peak failure (Okubo and Nishimatsu, 1985; Jansen and Shah, 1997). Two linear variable differential transformers (LVDTs) for each axial and lateral direction were used to acquire data and control the test in the current study.

### **2.2 Experimental work and computer vision**

Two different types of experiments were conducted: 1) different material

compositions were examined using cement paste, mortar, and concrete specimens, 2) model concrete specimens were studied with different number of aggregates.

Cement paste, mortar, and concrete specimens that have the dimensions of 100x75x75-mm were cast. Water-cement ratios for all three cases were kept as 0.4. The contact area between specimens and loading platens should be treated carefully, since it affects the displacement measurement and fracture behavior of the specimens. Capping compounds, a method used extensively, introduces soft layers and changes the fracture patterns (Jansen et al, 1995). To reduce the uncertainty, all specimen surfaces were ground. The shear confinement from the loading platens introduces tri-axial stress state near the contact area resulting in well-known conical failure (Choi et al., 1996). Researchers have shown that significant axial stresses as well as large shear stresses exist along the edge of the specimen loading area (Shah et al., 1995). A thin lubricant layer, which is a mixture of stearic acid and petroleum jelly, and Teflon sheets were used to reduce the frictions.

Computer vision examines two specimen images that represent two different deformation levels. The relative distance between two selected local subimages is calculated using a image correlation scheme. A charge-coupled device was used to capture specimen images. The accuracy of the technique is about 0.014 pixels for the current system. It is strongly dependent on the testing conditions, image quality, and specimen size.

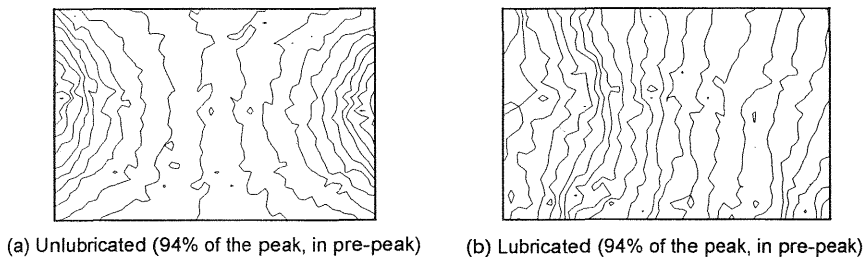


Fig. 1. Lateral displacement contours(5 microns/line, 100x75-mm)

### 2.3 Fracture of cement-based materials

When mortar specimens were tested under different end conditions, barrel shaped deformation was observed in case of high shear confinement as shown in Fig. 1a. The middle of the specimen deformed by about 100  $\mu\text{m}$ . The deformations near the top and bottom platens were about 30-40  $\mu\text{m}$ . When the shear constraint was reduced using a friction-reducing material, specimen deformed by 90-100  $\mu\text{m}$  over the specimen height (Fig. 1b). But

the deformations in Fig. 1b are not quite uniform due to the material heterogeneity, and it becomes clear in Fig. 2. Fig. 2 represents lateral deformation contours in three different materials: cement paste, mortar, and concrete specimens. They were tested under the same lubricated end condition. The deformation in cement paste, which is relatively homogeneous comparing other ones, was pretty uniform. On the other hand, concrete showed complex strain patterns due to large aggregates. The resolutions of the contour lines both in Fig. 1 and Fig. 2 are 5  $\mu\text{m}$ .

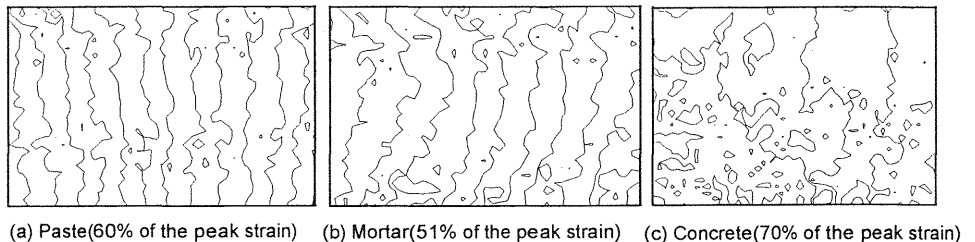


Fig. 2. Lateral displacement contours(pre-peak, 5 microns/line, 100x75-mm)

### 3 Fracture of concrete for different aggregate spacing

#### 3.1 Subregion scanning computer vision

Due to large aggregates in concrete specimens, the dimension of the specimens can not be smaller than the characteristic representative size. The computer vision methods described in the previous section was not sensitive enough to measure microcracks without reducing the observable region. Instead of the reducing viewing area, the technique was improved dramatically in accuracy by dividing the image into 8x7 subregions and increasing image resolution. In this method, which was named as subregion scanning computer vision (SSCV), the whole specimen viewing area was divided into fifty six subregions, and the digital CCD was aligned to cover only one subregion. The CCD system was moved over the specimen motorized transitional precision stages to capture all subimages from the whole specimen area. The average and standard deviation of the measurement errors with the current setup were estimated as about 0.65 and 0.45  $\mu\text{m}$ , respectively.

#### 3.2 Fracture of concrete with different aggregate contents

As shown in a previous section, the compositional quality of concrete dominates the failure mode of specimens. Formation of more vertically oriented - to the loading direction - cracks was observed in cement paste or mortar than in concrete. The sizes of cracks observed around peak loads

were smaller in concrete than in mortar or cement paste, and cracks were more evenly distributed in concrete. In this section, the initiation and propagation of cracks, which are essential to understand fundamental failure mechanism of concrete, is closely examined in conjunction with the effect of aggregate contents (or aggregate spacing). Three different types of specimens were prepared to examine the effect of aggregate spacing. Specimens that contain 1, 5, and 13 limestone aggregates were prepared (Fig. 3). The mix design for the mortar area was cement:find sand:water=1:1.27:0.45. Specimen size was 75x75x25-mm (width x height x thickness), and surfaces were ground and friction-reducing materials were used on the loading areas.

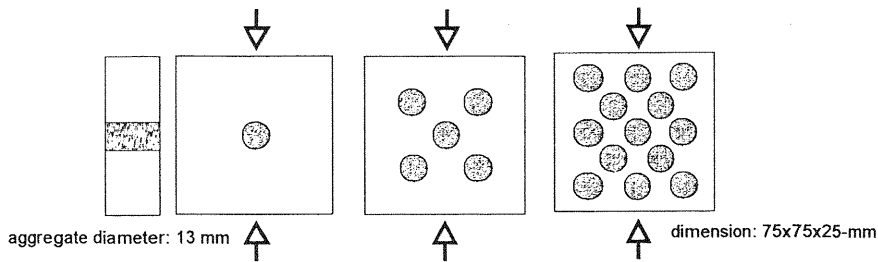


Fig. 3. Model concrete specimens containing various number of aggregates

The stress-strain curves are given in Fig. 4. Each step that reveals the relaxation of concrete is the period for image scanning. The feedback signal during the scanning session was kept constant to restrain crack propagation. The lateral displacement contours of 5 aggregate case, which was obtained using SSCV, provided precise microcrack development (Fig. 5). Model concrete which has 5 aggregates showed more evenly distributed cracks comparing 13 aggregate case. Near the peak load, each group of cracks starts connecting each other forming a global failure bands. If aggregates locate far enough, cracks propagate vertically in the matrix area and do not follow aggregate interfaces. It was observed, in the final failure patterns, that cracks were well distributed over the tested specimens forming vertical (loading direction) cracks in the mortar area and inclined cracks around aggregates.

#### 4 Discussion and conclusion

Regardless of the end conditions, material composition introduces nonlinearity in the pre-peak strains. Aggregate spacing changes the failure mechanism and there exists an optimum spacing which introduces better

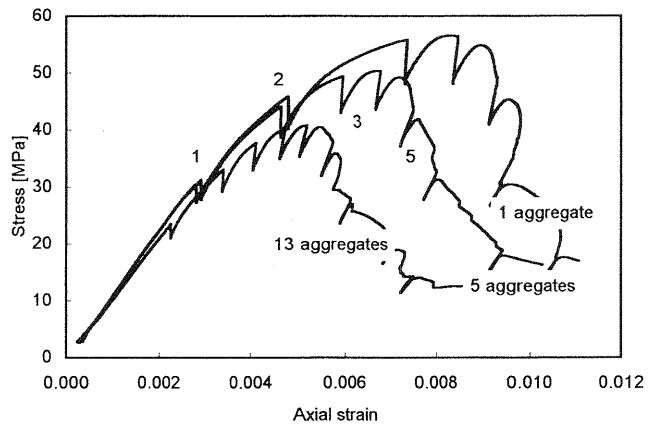


Fig. 4. Stress-strain curves with 3 different aggregate contents

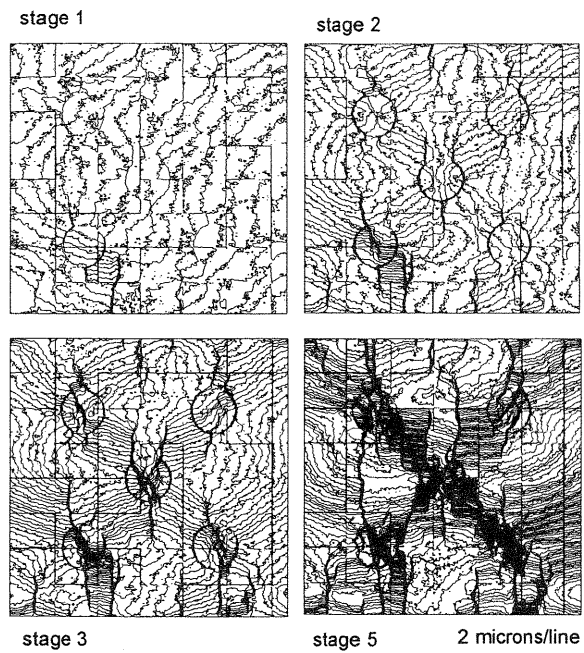


Fig. 5. Crack development in a 5\_aggregate specimen

stress redistribution during failure and, consequently, more uniform failure over the whole specimen area. The newly developed subregion scanning computer vision system (SSCV) provided accurate readings of microcrack openings over the whole specimen. SSCV will be particularly valuable for making inferences on microscopic damage and localization phenomena. However, there is considerable interest in the development of nondestructive methods to evaluate the condition of in-service structures. With the knowledge of basic fracture properties, relationships with a variety of NDE parameters can be established, and field tests can be developed. Evaluating distributed damage in reinforced concrete bridge decks, monitoring of fracture of bridge decks, and damage detection of structures that are remotely located will be promising applications for the current techniques.

## 5 Acknowledgment

The authors would like to acknowledge the financial support of the National Science Foundation Center for Science and Technology of Advanced Cement-Based Materials (ACBM), and U.S. Air Force Office of Scientific Research (AFOSR).

## 6 References

- Choi, S. and Shah, S.P. (1997) Deformation measurement in concrete under compression using image correlation. **Journal of Experimental Mechanics**, 37(3), 307-313.
- Choi, S. and Shah, S.P. (1998) Fracture mechanism in cement-based materials subjected to compression. **Journal of Engineering Mechanics**, 124(1), 94-102.
- Choi, S., Thienel, K.-C. and Shah, S.P. (1996) Strain softening of concrete in compression under different end constraints. **Magazine of Concrete Research**, 48(175), 103-115.
- Hillerborg, A. (1989) Stability problems in fracture mechanics testing. **Fracture of Concrete and Rock : Recent Developments** (eds. S.P. Shah, S. E. Swartz and B. Barr), 369-378.
- Hudson, J.A., Crouch, S.L. and Fairhurst, C. (1972) Soft, stiff and servo-controlled testing machines: A review with reference to rock failure. **Engineering Geology**, 6(3), 155-189.

- Jansen, D.C. and Shah, S.P. (1997) Effect of length on compressive strain softening of normal and high strength concrete. **Journal of Engineering Mechanics**, 123(1), 25-35.
- Jansen, D.C., Shah, S.P. and Rossow, E.C. (1995) Stress strain results of concrete from circumferential strain feedback control testing. **ACI Materials Journal**, 92(4), 419-428.
- Jia, Z. and Shah, S.P. (1994) Two-dimensional electronic speckle pattern interferometry and concrete fracture processes. **Experimental Mechanics**, 34(3), 262-270.
- Maji, A.K., Tasdemir, M.A. and Shah, S.P. (1991) Mixed mode crack propagation in quasi-brittle materials. **Engineering Fracture Mechanics**, 38(2/3), 129-145.
- Okubo, S. and Nishimatsu, Y. (1985) Uniaxial compression testing using a linear combination of stress and strain as the control variable. **International Journal of Rock Mechanics and Mining Sciences & Geomechanics Abstracts**, 22(5), 323-330.
- Shah, S.P., Choi, S. and Jansen, D.C., (1995) Strain softening of concrete in compression, in **Fracture Mechanics of Concrete Structures** (eds. Folker H. Wittmann), The Second International Conference on Fracture Mechanics of Concrete Structures (FRAMCOS2), ETH, Zurich, Switzerland, 1827-1841.
- Shao, Y., Li, Z. and Shah, S.P. (1993) Matrix cracking and interface debonding in fiber-reinforced cement-matrix composites. **Journal of Advanced Cement-Based Materials**, 1(2), 55-66.
- Wang, F., Shah, S.P. and Naaman, A.E. (1978). Stress-strain curves for normal and lightweight concrete in compression. **Journal of American Concrete Institute**, pp. 603-611.